Journal of Thermal Analysis and Calorimetry, Vol. 90 (2007) 2, 541–547

INVESTIGATION ON THE THERMAL DECOMPOSITION SOME HETERODINUCLEAR Ni^{II}–M^{II} COMPLEXES PREPARED FROM ONNO TYPE REDUCED SCHIFF BASE COMPOUNDS (M^{II}=Zn^{II}, Cd^{II})

M. Aksu[1], *S. Durmuş*[2], *M. Sari*[3], *K. C. Emregül*[4], *I. Svoboda*[5], *H. Fuess*[5] *and O. Atakol*[4*]

[1]Erciyes University, Yozgat Faculty of Science and Literature, Department of Chemistry, Yozgat Turkey
[2]Abant İzzet Baysal University, Faculty of Education, Bolu, Turkey
[3]Gazi University, Faculty of Education, Beşevler Ankara, Turkey
[4]Ankara University, Science Faculty, Department of Chemistry, Tandoğan 06100 Ankara, Turkey
[5]Strukturforschung, FB Materialwissenschaft, TU-Darmstadt Petersenstrasse 23, 64287 Darmstadt, Germany

N,N'-bis(salicylidene)-1,3-propanediamine (LH_2), N,N'-bis(salicylidene)-2,2'-dimethyl-1,3-propanediamine ($LDMH_2$), N,N'-bis(salicylidene)-2-hydroxy-1,3-propanediamine (LOH_3), N,N'-bis(2-hydroxyacetophenylidene)-1,3-propanediamine ($LACH_2$) and N,N'-bis(2-hydroxyacetophenone)-2,2'-dimethyl-1,3-propanediamine ($LACDMH_2$) were synthesized and reduced to their phenol-amine form in alcoholic media using $NaBH_4$ (L^HH_2, LDM^HH_2, LOH^HH_2, LAC^HH_2 and $LACDM^HH_2$). Heterodinuclear complexes were synthesized using Ni(II), Zn(II) and Cd(II) salts, according to the template method in DMF media.

The complex structures were analyzed using elemental analysis, IR spectroscopy, and thermogravimetry. Suitable crystals of only one complex were obtained and its structure determined using X-ray diffraction, $NiLAC^H{\cdot}CdBr_2{\cdot}DMF_2$, space group orthorhombic, Pbca, a=20.249, b=14.881, c=20.565 Å and Z=8. The heterodinuclear complexes were seen to be of [$Ni{\cdot}ligand{\cdot}MX_2{\cdot}DMF_2$] structure (ligand=$L^{H2-}$, LDM^{H2-}, LOH^{H2-}, LAC^{H2-}, $LACDM^{H2-}$, M=Zn^{II}, Cd^{II}, X=Br^-, I^-). Thermogravimetric analysis showed irreversible bond breakage of the coordinatively bonded DMF molecules followed by decomposition at this temperature.

Keywords: *crystal structure, heterodinuclear complexes, ONNO type Schiff bases, thermal analysis*

Introduction

N,N'-bis(salicylidene)-1,3-propanediamine (LH_2), is known to give dinuclear and trinuclear complexes since 1976 and 1990, respectively [1, 2]. The formation of tetra- and polynuclear complexes have also been reported by many authors [3–7]. Compounds containing iminic bonds are known to give hydrolysis reactions in amfiprotic media. On this account these types of compounds are reduced to their amine forms and hydrolyis is prevented at the cost of change in the ligand characteristics [5, 6, 8, 9].

In this study 5 ONNO type Schiff base compounds were derived from salicyaldehyde, 2-hydroxyacetophenone, 1,3-propanediamine, 2-hydroxy-1,3-propanediamine and 2,2'-dimethyl-1,3-propanediamine and reduced with $NaBH_4$ in alcoholic media (Fig. 1). Ni^{II}–Zn^{II} and Ni^{II}–Cd^{II} complexes of these ligands were prepared in DMF media according to the template method (Fig. 2). Only one structure gave appropriate crystals for X-ray analysis. C, H, N, Ni and halogen analysis was performed for all crystals. The thermal decomposition of the crystals were studied thermogravimetrically.

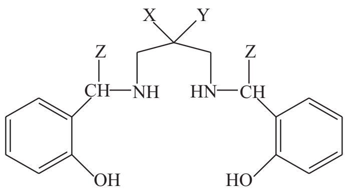

X=Y=Z=H	L^HH_2
X=Z=H Y=OH	LOH^HH_2
Z=H X=Y=CH_3	LDM^HH_2
Z=CH_3 X=Y=H	LAC^HH_2
X=Y=Z=CH_3	$LACDM^HH_2$

Fig. 1 Chemical formulas of the ligands

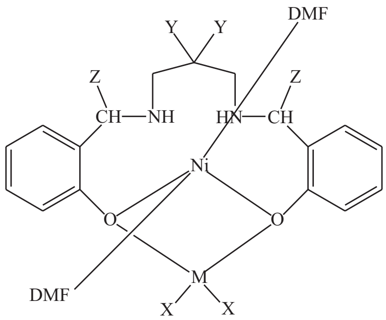

Y, Z=H, CH_3, OH
X=Br^-, I^-
M=Cd^{2+}, Zn^{2+}

Fig. 2 Chemical formulas of the complexes

---

[*] Author for correspondence: atakol@science.ankara.edu.tr

1388–6150/$20.00

Akadémiai Kiadó, Budapest, Hungary
Springer, Dordrecht, The Netherlands

Experimental

Materials

Preparation of the ligands

The Schiff base compounds, N,N'-bis(salicylidene)-1,3-propanediamine (LH_2),
N,N'-bis(salicylidene)-2,2'-dimethyl-1,3-propanediamine ($LDMH_2$),
N,N'-bis(salicylidene)-2-hydroxy-1,3-propanediamine (LOH_3),
N,N'-bis(2-hydroxyacetophenylidene)-1,3-propanediamine ($LACH_2$) and
N,N'-bis(2-hydroxyacetophenone)-2,2'-dimethyl-1,3-propanediamine ($LACDMH_2$) were synthesized from the aldehyde components, salicylaldehyde and 2-hydroxyacetophenone, and the amine components, 1,3-propanediamine 2,2'-dimethyl-1,3-propanediamine and 2-hydroxy-1,3-propanediamine in ethanol. The reduced compounds, L^HH_2, LDM^HH_2, LOH^HH_2, LAC^HH_2 and $LACDM^HH_2$ were prepared according to the following procedure [8].

0.05 moles of LH_2, $LDMH_2$ and LOH_3 were dissolved in 100 mL of MeOH, whereas $LACH_2$ and $LACDMH_2$ were dissolved in a 1:2 mixture of 2-Pr-OH:MeOH. Small portions of $NaBH_4$ were added and stirred until the solution was colorless. To this solution was added ice and twice its volume of water. The mixture was left to stand for 1–2 days and the resulting precipitate was filtered. The yield% and melting points are given in Table 1.

Table 1 Yield% and melting points of the reduced ligands

Ligand	Yield %	Melting point/°C
L^HH_2	87	106–108
LDM^HH_2	91	95–96
LOH^HH_2	56	77–79
LAC^HH_2	90	114–116
$LACDM^HH_2$	92	89–91

Preparation of the complexes

All complexes were prepared as template according to the following procedure.

0.0014 moles of the reduced ligands, L^HH_2, LDM^HH_2, LOH^HH_2, LAC^HH_2 and $LACDM^HH_2$ were dissolved in 30 mL hot DMF (as these are equilibrium reactions increased amounts of the ligand in comparison to the stoichiometric amounts increases the yield). To this solution was added 0.25 mL of triethanolamine and the solutions of 0.001 moles (0.237 g) $NiCl_2·6H_2O$ in 20 mL of methanol and ZnX_2 or CdX_2 (X=$Br^–$, $I^–$) in 20 mL of methanol. The solutions were left to stand for 4–5 days and the resulting blue colored crystals were filtered and dried in air.

Methods

Elemental analysis was performed on a Eurovector 3018 C,H,N,S analyzer instrument. Nickel analysis was done gravimetrically using dimethylglyoxime, whereas other metal analysis was performed on a Hitachi 8200 model atomic adsorption spectrometer. Halogen analysis was performed gravimetrically using $AgNO_3$. IR spectra were obtained on a Mattson FTIR 1000 instrument using the KBr disk technique.

TG-DTA curves were obtained using a Shimadzu TG-60H instrument. Platinum pans were used for thermograms obtained between room temperature and 850°C. The curves were obtained under nitrogen atmosphere with a flow rate of 100 mL $min^{–1}$. The heating rate was 10°C $min^{–1}$ for the curves obtained between room temperature and 750°C.

Data were collected on an Oxford Diffraction Xcalibur$^{(TM)}$ Single Crystal X-ray Diffractometer [10] with MoK_α radiation using $\omega/2\theta$ scan mode. Unit cell parameters were refined from the setting angles of 25 centered reflections in the range of (I) $4.09 \leq \theta \leq 26.37$. Three standard reflections for every 120 min during data collection showed no significant intensity variations. The structures were solved by a combination of direct methods and Fourier techniques and refined by full-matrix least squares using the solution program SHELXS97 [11] in the WinGX package [12] and refined using SHELXL97 [11].

In the structure, the C18 atom is disordered. The disorder of atoms C18a and C18b was refined, with occupancies of 0.60(2) and 0.40(2), respectively. H atoms on N1 and N2 were located in a difference Fourier map and refined isotropically. Other H atoms

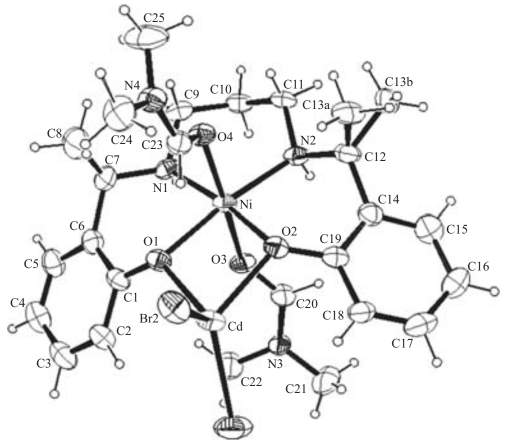

Fig. 3 The molecular structure and atomic labeling scheme of the complex $NiL^H·CdBr_2·DMF_2$. Displacement ellipsoids are drawn at the 40% probability level

were placed geometrically (C–H=0.93 and 0.97 Å) based on their parent C atoms and riding model was used for H atoms, with $U_{iso}(H)=1.2U_{eq}(C,N)$, or $1.5U_{eq}(C)$ for methyl atoms.

Results and discussion

The ORTEP drawing [13] of the molecular structure and atomic labeling scheme of $NiL^{H}{\cdot}CdBr_2{\cdot}DMF_2$ is shown in Fig. 3. Crystallographic and experimental data for the complex is given in Table 2 and selected bond lengths and angles are given in Table 3. Elemental analysis results and important IR data are given in Tables 4 and 5, respectively. Thermoanalytical data are summarized in Table 6.

X-ray studies show the $NiLAC^{H}{\cdot}CdBr_2{\cdot}DMF_2$ complex to be dinuclear in structure. All other elemental analysis results obtained for other complexes showed similarity with that obtained for $NiLAC^{H}{\cdot}CdBr_2{\cdot}DMF_2$, from which we can assume that all other structures are also dinuclear in structure. Thermogravimetric analysis is as useful a method as element analysis in determination of the complex stoichiometry. In fact, determining the mass loss due to thermal separation of small ligands is sometimes even a better method than element analysis [14]. There are two DMF molecules coordinated by the Ni(II) ion in the complex structure. Thermogravimetrically, appropriate mass loss coinciding with the separation of these two molecules should be observed. Examples of some TG curves are given in Figs 4 and 5. It is difficult to identify the DMF separation reaction from these curves. The DMF mass loss can partially be detected from the curves of the Ni^{II}–Cd^{II} complex structures (Fig. 4) whereas it is extremely difficult with the curves of the Ni^{II}–Zn^{II} complex structures (Fig. 5).

The mass loss between 13.4 and 20.8% in the range 141–283°C is probably due to the loss of the two DMF molecules (Fig. 4). On the other hand, it is very difficult to establish this range from the thermograms of the Ni^{II}–Zn^{II} complexes (Fig. 5). This is because Zn is both a hard ion and attracts electrons

Table 2 Crystallographic and experimental data for the complex

Chemical formula	$C_{25}H_{38}Br_2CdN_4NiO_2$
Formula mass	789.52
Temperature/K	299(2)
Wavelength/Å	0.71073
Crystal system, space group	orthorhombic, Pbca
Unit cell dimensions: (Å, °)	
a	20.249(2)
b	14.881(2)
c	20.565(10)
Volume/$Å^3$	6196.8(11)
Z	8
Calculated density/Mg m^{-3}	1.693
Absorption coefficient/mm^{-1}	3.908
F(000)	3152
Crystal size/mm	0.50x0.16x0.12
$2\theta_{max}$/°	52.74
Index range	$-25\leq h\leq 25$, $-9\leq k\leq 18$, $-25\leq l\leq 25$
Number of reflections used	3277 $(I\geq 2\sigma(I))$
Number of parameters	352
R_{int}	0.053
R	0.049
R_w	0.135
Goodness of fit	1.013
$\Delta\rho_{min}$, $\Delta\rho_{max}$/e $Å^{-3}$	–0.673, 0.751

Table 3 Selected bond lengths (Å) and angles (°)

Ni	N1	2.101(6)	
Ni	N2	2.085(5)	
Ni	O1	2.069(4)	
Ni	O2	2.067(4)	
Ni	O3	2.115(4)	
Ni	O4	2.084(4)	
O1	Cd	2.216(4)	
O2	Cd	2.226(4)	
Br1	Cd	2.525(10)	
Br2	Cd	2.540(10)	
Ni	O1	Cd	100.03(16)
Ni	O2	Cd	99.81(16)
O2	Ni	O1	83.11(15)
O2	Ni	O4	91.90(15)
O1	Ni	O4	94.19(15)
O2	Ni	N2	90.93(18)
O1	Ni	N2	172.75(18)
O2	Ni	N1	172.4(2)
O1	Ni	N1	89.3(2)
N2	Ni	N1	96.6(2)
O4	Ni	O3	174.50(16)
N2	Ni	O3	89.01(19)
O1	Cd	O2	76.29(14)
O1	Cd	Br1	121.14(10)
O2	Cd	Br1	120.08(11)
O1	Cd	Br2	109.26(10)
O2	Cd	Br2	108.48(10)
Br1	Cd	Br2	115.35(4)

Table 4 Elemental analysis results

Complex	Expected/%					Found/%				
	C	H	N	Ni	X (Br, I)	C	H	N	Ni	X (Br, I)
$NiL^H·ZnBr_2·DMF_2$	38.67	4.79	7.82	8.22	22.37	38.49	5.06	7.76	8.18	23.42
$NiL^H·ZnI_2·DMF_2$	34.16	4.24	6.92	7.26	31.41	33.88	5.04	7.31	7.38	33.04
$NiL^H·CdBr_2·DMF_2$	36.28	4.50	7.35	7.71	20.99	35.59	4.41	7.54	7.70	21.86
$NiL^H·CdI_2·DMF_2$	32.39	4.00	6.55	6.86	29.70	33.01	3.91	6.08	7.10	30.43
$NiLDM^H·ZnBr_2·DMF_2$	40.44	5.16	7.54	7.90	21.52	39.16	4.52	7.40	7.88	22.03
$NiLDM^H·ZnI_2·DMF_2$	35.88	4.57	6.69	7.01	30.36	35.49	4.11	6.42	6.73	31.44
$NiLDM^H·CdBr_2·DMF_2$	38.03	4.85	7.09	7.43	20.24	38.27	4.62	7.24	7.58	22.13
$NiLDM^H·CdI_2·DMF_2$	33.97	4.33	6.34	6.64	28.77	33.14	4.04	6.76	6.51	29.38
$NiLOH^H·ZnBr_2·DMF_2$	37.82	4.69	7.66	8.03	21.88	38.42	4.99	7.28	8.07	22.91
$NiLOH^H·ZnI_2·DMF_2$	33.49	4.16	6.79	7.12	30.80	33.36	4.77	6.94	7.33	33.46
$NiLAC^H·ZnBr_2·DMF_2$	40.44	5.16	7.54	7.90	21.52	41.09	5.27	7.41	8.07	22.15
$NiLAC^H·ZnI_2·DMF_2$	35.88	4.57	6.69	7.01	30.36	34.90	4.83	6.57	7.17	31.01
$NiLAC^H·CdBr_2·DMF_2$	38.03	4.85	7.09	7.43	20.24	38.12	5.62	7.47	7.91	21.03
$NiLAC^H·CdI_2·DMF_2$	33.97	4.33	6.34	6.64	28.77	33.65	4.21	6.56	6.72	28.92
$NiLACDM^H·ZnBr_2·DMF_2$	42.08	5.49	7.27	7.62	20.74	42.51	5.74	7.96	7.78	21.04
$NiLACDM^H·ZnI_2·DMF_2$	37.50	4.89	6.48	6.79	29.37	36.84	4.35	6.43	7.03	31.17
$NiLACDM^H·CdI_2·DMF_2$	35.56	4.64	6.14	6.44	27.86	34.91	4.46	6.37	6.58	28.64

$NiLOH^H·CdBr_2·DMF_2$ and $NiLOH^H·CdI_2·DMF_2$ could not be isolated

very effectively [15]. Cd, on the other hand is a soft ion. Due to its weaker electron accepting nature, it attracts the phenolic oxygen weakly with respect to the Zn ion, leading to the formation of weaker coordinative bonds between the Ni(II) ions and the DMF molecules. In the case of Zn(II), stronger Ni(II) DMF coordination bonds are formed. In previous studies the Ni–O (DMF) bond lengths were found to be shorter in the Ni^{II}–Zn^{II} complexes with respect to the Ni^{II}–Cd^{II} complexes [16–18]. Due to the strong coordination of the DMF molecules in the Ni^{II}–Zn^{II} complexes, the temperature at which thermal decomposition begins is in the range 160–240°C, and ends within a range of 110°C, depending on the ligand. Although it is difficult to observe this from the curves, loss of DMF molecules ends between 265–365°C, depending on the ligand. The DMF molecules seem to be situated in the coordinated structure until decomposition begins. The DTG peaks for L^H and LDM^H were observed above 240°C, between 210–220°C for

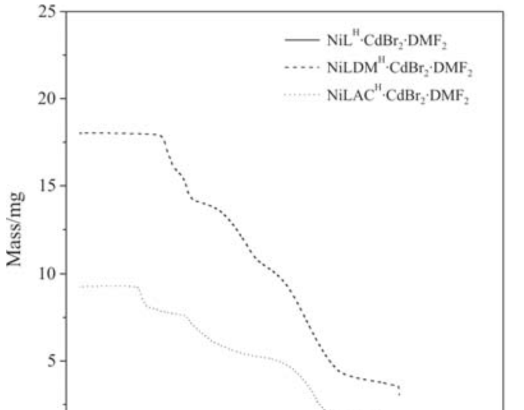

Fig. 4 TG curves of some Ni^{II}–Cd^{II} complexes

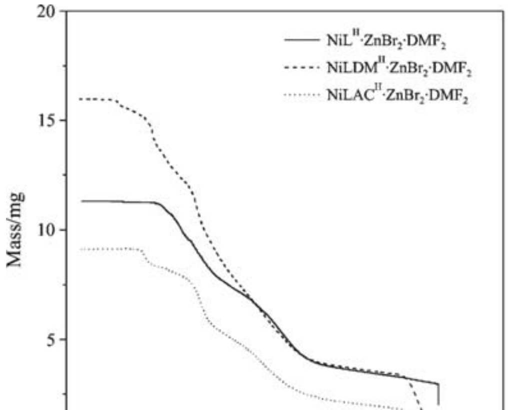

Fig. 5 TG curves of some Ni^{II}–Zn^{II} complexes

Table 5 Important IR data

Ligand/complex	IR data/cm^{-1}						
	$\nu_{N–H}$	$\nu_{C–H}$ aromatic	$\nu_{C–H}$ aliphatic	$\nu_{C=O}$ DMF	$\nu_{C=C}$	δ_{CH_2}	$\delta_{C–H}$ aromatic
$L^{H}H_2$	3289	3051–3072	2931–2826	–	1596	1469	758
$LDM^{H}H_2$	3293	3049–3074	2956–2855	–	1592	1468	759
$LOH^{H}H_2$	3259	3053–3080	2971–2854	–	1590	1470	758
$LAC^{H}H_2$	3290	3050–3068	2925–2856	–	1598	1470	757
$LACDM^{H}H_2$	3277	3049–3071	2925–2856	–	1596	1471	758
$NiL^{H}\cdot ZnBr_2\cdot DMF_2$	3252–3218	3053–3012	2928–2863	1662	1598	1487	761
$NiL^{H}\cdot ZnI_2\cdot DMF_2$	3253–3220	3055–3011	2925–2864	1657	1595	1473	759
$NiL^{H}\cdot CdBr_2\cdot DMF_2$	3252–3219	3060–3007	2925–2863	1658	1595	1475	757
$NiL^{H}\cdot CdI_2\cdot DMF_2$	3252–3217	3061–3013	2929–2863	1664	1597	1485	758
$NiLDM^{H}\cdot ZnBr_2\cdot DMF_2$	3252–3218	3059–3011	2928–2859	1660	1595	1481	757
$NiLDM^{H}\cdot ZnI_2\cdot DMF_2$	3252–3220	3062–3009	2928–2860	1659	1596	1482	758
$NiLDM^{H}\cdot CdBr_2\cdot DMF_2$	3250–3217	3065–3007	2933–2864	1661	1595	1477	757
$NiLDM^{H}\cdot CdI_2\cdot DMF_2$	3251–3218	3061–3008	2929–2858	1660	1597	1475	761
$NiLOH^{H}\cdot ZnBr_2\cdot DMF_2$	3259–3226	3057–3003	2928–2860	1658	1595	1473	758
$NiLOH^{H}\cdot ZnI_2\cdot DMF_2$	3260–3230	3057–3001	2926–2863	1657	1595	1475	760
$NiLAC^{H}\cdot ZnBr_2\cdot DMF_2$	3252–3218	3060–3007	2928–2861	1661	1593	1475	758
$NiLAC^{H}\cdot ZnI_2\cdot DMF_2$	3253–3216	3059–3011	2927–2863	1658	1596	1481	758
$NiLAC^{H}\cdot CdBr_2\cdot DMF_2$	3254–3220	3059–3012	2927–2836	1660	1596	1479	758
$NiLAC^{H}\cdot CdI_2\cdot DMF_2$	3255–3219	3060–3006	2928–2860	1660	1594	1480	757
$NiLACDM^{H}\cdot ZnBr_2\cdot DMF_2$	3275–3236	3051–3017	2924–2863	1652	1596	1489	758
$NiLACDM^{H}\cdot ZnI_2\cdot DMF_2$	3279–3233	3052–3018	2925–2821	1650	1596	1490	759
$NiLACDM^{H}\cdot CdI_2\cdot DMF_2$	3254–3220	3053–3017	2925–2820	1648	1597	1485	757

LAC^{H} and at approximately 190°C for $LACDM^{H}$. It has previously been reported that the L^{H} and LDM^{H} begin decomposing above 250°C [14]. As decomposition begins before the DMF molecules totally leave the structure determination of the DMF mass is almost impossible. Decomposition of the complexes with LAC^{H}, $LACDM^{H}$ and LOH^{H} ligands begin at lower temperatures than the complexes formed with the L^{H} and LDM^{H} ligands. It has previously been reported that CH_3 and OH groups decrease the decomposition temperatures [14]. In addition, the decomposition temperatures of $NiLOH^{H}\cdot ZnBr_2\cdot DMF_2$ and $NiLOH^{H}\cdot ZnI_2\cdot DMF_2$ were found to be extremely low with values of 93 and 117°C.

The first thermal decomposition reaction of the Ni^{II}–Cd^{II} complexes are seen to be scattered at various temperature ranges; 190–280°C for L^{H} complexes, 150–270°C for LDM^{H} complexes, 104–205°C for LAC^{H} complexes and 140–220°C for $LACDM^{H}$ complexes. Ni^{II}–Cd^{II} complexes of LOH^{H} were not able to be isolated. The important fact that should be noticed is that the first thermal decomposition reaction of the Ni^{II}–Cd^{II} complexes begins at lower temperatures than the Ni^{II}–Zn^{II} complexes. This shows that the Cd(II) ion attracts less electrons over the μ-bridges with respect to the Ni(II) ion. As a result, a weaker bond between the Ni(II) ion and DMF molecules is formed leading to an easier thermal reaction.

The initiation of a second thermal decomposition reaction can be observed above 260°C which lasts upto 650°C for all complexes under study. Previous studies have reported NiO as residue for Ni(II)–Schiff base complexes at about 650°C [19, 20]. The total mass loss observed above 650°C for L^{H} and LDM^{H} complexes, LAC^{H} complexes $LACDM^{H}$ complexes is in the range of 65–70, 70–72 and 75%, respectively. The amounts of residue found are lower than the expected stochiometric amounts coinciding with $NiO+ZnX_2$ and $NiO+CdX_2$. The melting points of $ZnBr_2$, ZnI_2, $CdBr_2$ and CdI_2 are given as 394, 446, 567 and 387°C, respectively [21]. These compounds are quite volatile within the studied temperature range and partial evaporation can be expected. As a result all of the halide compounds will not be found in the residue. Purging of oxygen into the media at 650 or 750°C gives rise to a violent exothermic reaction in all curves. After these reactions a residue in the range of 6.5–11% is seen to remain, which coincides with the expected NiO amounts. This shows probable

Table 6 Thermoanalytical data

Complex	First thermal reaction DMF loss				Second thermal reaction thermal decomposition	
	Temperature range/°C		Expected mass loss/%	Found mass loss/%	Temperature range/°C	Found mass loss/%
NiL^{H}·ZnBr$_2$·DMF$_2$	209–324	DTA peak 246	20.43	n/a	338–670	43.33
NiL^{H}·ZnI$_2$·DMF$_2$	209–306	DTA peak 239	18.56	n/a	331–650	41.56
NiL^{H}·CdBr$_2$·DMF$_2$	191–283	DTA peak 240	19.17	20.81	267–640	43.86
NiL^{H}·CdI$_2$·DMF$_2$	204–248	DTA peak 217	17.06	19.59	285–650	44.27
NiLDM^{H}·ZnBr$_2$·DMF$_2$	246–365	DTA peak 263	19.66	n/a	340–660	42.80
NiLDM^{H}·ZnI$_2$·DMF$_2$	234–355	DTA peak 247	17.49	n/a	340–650	44.17
NiLDM^{H}·CdBr$_2$·DMF$_2$	146–240	DTA peak 178	18.49	16.88	260–665	44.46
NiLDM^{H}·CdI$_2$·DMF$_2$	175–270	DTA peak 227	16.52	15.85	300–670	44.83
NiLOH^{H}·ZnBr$_2$·DMF$_2$	117–280	DTA peak 151	19.98	18.34	290–685	53.09
NiLOH^{H}·ZnI$_2$·DMF$_2$	93–222	DTA peak 122	17.70	n/a	245–675	64.18
NiLAC^{H}·ZnBr$_2$·DMF$_2$	143–230	DTA peak 217	19.66	24.85	240–360	51.87
NiLAC^{H}·ZnI$_2$·DMF$_2$	135–245	DTA peak 218	17.49	20.64	250–620	55.89
NiLAC^{H}·CdBr$_2$·DMF$_2$	137–265	DTA peak 178	18.49	17.78	260–640	55.35
NiLAC^{H}·CdI$_2$·DMF$_2$	164–205	DTA peak 184	16.52	15.49	270–675	53.02
NiLACDM^{H}·ZnBr$_2$·DMF$_2$	166–265	DTA peak 190	18.94	13.41	270–660	61.83
NiLACDM^{H}·ZnI$_2$·DMF$_2$	162–275	DTA peak 188	16.88	n/a	280–660	59.18
NiLACDM^{H}·CdI$_2$·DMF$_2$	141–224	DTA peak 73	16.01	15.94	250–660	60.22

n/a – not available

carbonization during the first and second thermal decomposition reactions. We can conclude in the light of all the present data that the residue at 650°C is composed of NiO, some left over halide compounds and carbonized material. Literature has proven transition metal complexes of ONO or ONNO type Schiff base compounds to form metal oxides above 650°C [19, 20].

The Ni(II) ion shows a deformed octahedral coordination structure within the complexes, whereas Cd^{II} and Zn^{II} show deformed tetrahedral coordinations. The ORTEP drawing of the molecular structure of NiL^{H}·CdBr$_2$·DMF$_2$ is shown in Fig. 3. The Ni(II) ion is situated between the two oxygen and nitrogen donors of the organic ligand and the oxygen atoms of the DMF molecules within an O$_4$N$_2$ coordination sphere. Cd(II), on the other hand is situated in an O$_2$Br$_2$ coordination sphere. A similar structure has previously been reported in literature [22]. The O$_2$N$_2$ donor atoms of the organic ligand constitute the basal plane, whereas the oxygen atoms of the DMF molecules are in apical position. The longest bond lengths are found between the Ni ion and the DMF oxygens, with values of 2.119 and 2.087 Å, whereas the largest angle is the O3–Ni–O4 angle with a value of 174.56°. The NiN1C8C9C10N2 chelate ring is in the chair conformation as expected. The angles between the N1C8C10N2 plane and the N1NiN2 and C8C9C10 planes are 28.47 and 64.79°, respectively.

The Br$_1$–Cd–Br$_2$ angle within the Cd(II) coordination is a little larger than an ideal tetrahedron, with a value of 119.37° and the angle between the Cd(II) ion and the phenolic oxygen is 76.30°. As the phenolic oxygens tend to form bonds with group IIB elements via μ-bridges the angles in general are small [22, 23].

Supplementary materials

Crystallographic data for the structural analysis have been deposited with the Cambridge Crystallographic Data Center, CCDC 606868. Copies of this information can be obtained free of charge from The Director, CCDC, 12 Union Road, Cambridge, CB2, 1EZ, UK (fax +44-1223-336-033; e-mail: deposit@ccdc.cam.ac.uk or http://www.ccdc.cam.ac.uk).

Acknowledgements

Professor Orhan Atakol is A DAAD grantee and would like to thank Prof. Dr. HARTMUT FUESS for providing laboratory facilities. The authors also thank the Ankara University Scientific Research Fund (Project No: 20030705083) for their support.

References

1 R. J. Butcher and E. Sinn, Inorg. Chem., 15 (1976) 1604.
2 C. Fukuhara, K. Tsuneyoshi, N. Matsumoto, S. Kida, M. Mikuriya and M. Mori, J. C. S. Dalton Trans., Vol. (1990) 3473.
3 M. Mikuriya, N. Tsuru, S. Ikemi and S. Ikenova, Chem. Lett., (1998) 879.
4 K. J. Reddy, M. V. Rajasekharan and J. P. Tuchaques, Inorg. Chem., 37 (1998) 5978.
5 Y. Song, P. Gomez, O. Roubeau, I. Mutikainen, U. Terpeinen and J. Reedijk, Inorg. Chim. Acta, 358 (2005) 109.
6 Y. Song, C. Massera, P. Gomez, O. Roubeau, A. M. Manotti Lanfredi and J. Reedijk, Inorg. Chem., 43 (2004) 6842.
7 R. Kurtaran, Kaan.C. Emregül, C. Arıcı, F. Ercan, V. J. Catalano and O. Atakol, Synth. React. Inorg. Met.-Org. Chem., 33 (2003) 281.
8 H. Aneetha, K. Pannerselvam, T. F. Liao, T. H. Lu and C. S. Chung, JCS Dalton Trans., J. C. S. (1999) 2689.
9 S. Durmus, L. Tatar, C. Arici, N. Dinçer, O. Atakol, I. Svoboda and H. Fuess, Z. Kristallogr., 220 (2005) 977.
10 Oxford Diffraction (2002) CrysAlis CCD and CrysAlis RED. Version 1.170.14. Oxford Diffraction, Oxfordshire, England.
11 G.M. Sheldrick, SHELXS97 and SHEXL97. Program for Crystal Structure Solution and Refinement. University of Göttingen, Germany 1997.
12 L. J. Farrugia, WinGX. Program for Crystallography Package. J. Appl. Cryst., 32 (1999) 837.
13 A. L. Spek, PLATON, Program for Crystal Molecular Drawing. University of Utrecht, The Netherlands 2000.
14 S. Durmuş, Ü. Ergun, J. C. Jaud , K. C. Emregül, H. Fuess and O. Atakol, J. Therm. Anal. Cal., 86 (2006) 337.
15 R. G. Pearson, Inorg. Chem., 27 (1988) 734.
16 C. Arıcı, F. Ercan, R. Kurtaran and O. Atakol, Acta Cryst. Section C, C57 (2001) 812.
17 S. Durmuş, L. Tatar, Z. Durmuş, K. C. Emregül and O. Atakol, J. Inst. Sci. Technol., Gazi University, 14 (2001) 541.
18 M. Döring, G. Hahn and W. Imhof, Acta Cryst. Section E, E62 (2006) m429.
19 E. T. G. Cavalherio, F. C. D. Lemos, J. Z. Schpector and E. R. Dockal, Thermochim. Acta, 370 (2001) 129.
20 A. I. El-Said, J. Therm. Anal. Cal., 68 (2002) 917.
21 CRC Handbook of Chemistry and Physics, 64th Edition (1984), pp. B77, B155-B156.
22 L. Tatar, O. Atakol and C. Arıcı, Acta. Cryst. Section E, E58 (2002) m154.
23 İ. Ercan, F. Ercan, C. Arıcı and O. Atakol, Acta Cryst. Section C, 58 (2002) m137.

Received: May 31, 2006
Accepted: April 5, 2007
OnlineFirst: June 1, 2007

DOI: 10.1007/s10973-006-7729-5